Anisotropic thermal conductivity of natural Boom Clay

Linh Quyen Dao, Pierre Delage, Anh Minh A.M. Tang, Yu-Jun Cui, Jean-Michel Pereira, Xiang-Ling Li, Xavier Sillen

Anisotropic thermal conductivity of natural Boom Clay

Linh-Quyen DAO [1], Pierre DELAGE [1], Anh-Minh TANG [1], Yu-Jun CUI [1]

Jean-Michel PEREIRA [1], Xiang-Ling LI [2], Xavier SILLEN [3]

[1] *Ecole des Ponts ParisTech, UR Navier/CERMES, 6-8, av. Blaise Pascal, Cité Descartes, 77455 Marne-la-Vallée, France.*

[2] *European Underground Research Infrastructure for Disposal of nuclear waste in Clay Environment (EURIDICE, Mol, Belgium)*

[3] *Belgian Agency for Radioactive Waste and Enriched Fissile Materials (ONDRAF/NIRAS, Brussels, Belgium)*

Corresponding author:

Prof. Yu-Jun CUI

Ecole des Ponts ParisTech

6-8 av. Blaise Pascal, Cité Descartes, Champs-sur-Marne

77455 Marne-la-Vallée cedex 2

France

Email : yujun.cui@enpc.fr

Phone : +33 1 64 15 35 50

Fax : +33 1 64 15 35 62

Abstract

The thermal conductivity of host rocks is an important parameter in the design of deep geological disposal of heat-emitting radioactive waste. Due to bedding, heat transfer in sedimentary rocks is affected by their transversally isotropic structure. In this work, an experimental program is run to measure the thermal conductivities of Boom Clay along various orientations with respect to the bedding plane by using the needle thermal probe technique. Measurements were performed on specimens obtained from cores drilled from the HADES Underground Research Laboratory (URL) at Mol, Belgium, at a depth of 223 m. The thermal conductivities values obtained are in good agreement with those previously published, confirming the thermal anisotropy of the Boom Clay. Moreover, the observed changes in thermal conductivity with respect to the distance to the gallery provide further evidence on the extent of the Excavation Damaged Zone around the gallery.

Keywords: Thermal conductivity; Boom Clay; thermal anisotropy; excavation damaged zone; laboratory test.

1 Introduction

In the context of deep geological disposal of heat-emitting high activity radioactive waste, the thermal conductivity of the host geological formation (stiff clays, mudstones, granites, etc.) is an important

parameter in the design of the disposal. Moreover, the thermal transient phase that will be experienced by the system over hundreds to thousands of years after waste emplacement represents an important part of its long-term evolution (Yu et al., 2013). Due to a layered microstructure resulting from the initial deposition and further geological processes, stiff clays and claystones are known to preferentially conduct heat along the direction parallel to the bedding plane. Indeed, this anisotropy of thermal conductivity was observed in various stiff clays and claystones including the London clay, the Callovo-Oxfordian claystone (COx, East of France) and the Opalinus clay (Switzerland). In London clay, the thermal conductivity in the direction perpendicular to the bedding plane was found equal to 0.83 W/(m.K) whereas that in the direction parallel to the bedding plane was equal to 1.19 W/(m.K) (Midttømme and Roaldset, 1999). The thermal conductivity of Opalinus Clay was investigated by Mügler et al. (2006). They reported that the values obtained by in-situ back analysis are 0.55 - 1.07 W/(m.K) in the direction perpendicular to bedding and 1.84 - 1.90 W/(m.K) in the direction parallel to bedding, respectively. Buntebarth (2004) (in Jobmann and Polster, 2007) gave, from laboratory experiments, thermal conductivities of 0.75 W/(m.K) and 1.55 W/(m.K) for the directions perpendicular and parallel to bedding, respectively. The thermal conductivity in the direction perpendicular to the bedding plane of the COx claystone varies between 1.3 and 1.9 W/(m.K) whereas that in the direction parallel to the bedding plane varies between 1.9 and 2.7 W/(m.K) (ANDRA, 2005).

Based on the values in the two directions, a degree of thermal conductivity anisotropy (or anisotropy effect) η can be defined, as follows (Popov et al., 1999; Pribnow et al., 2000; Davis et al., 2007):

$$\eta = \frac{\lambda_{//}}{\lambda_{\perp}} \tag{1}$$

From the values of thermal conductivity introduced above, a value of η = 1.43 is determined for London clay. For Opalinus Clay and COx claystone, η can vary from 1.78 to 3.34 and from 1.42 to 1.46, respectively.

In Boom Clay, the anisotropy of thermal conductivity has been inferred through the back analysis of a small scale in-situ heating experiment, ATLAS III, carried out in the Underground Research Laboratory (URL) HADES at a depth of 223 m (Chen et al., 2011). The measurements of temperature evolution at different distances from the heater were compared with the results of heat transfer

simulations. In those simulations, adopting values of thermal conductivities equal to 1.65 W/(m.K) and 1.31 W/(m.K) for the directions parallel and perpendicular to the bedding plane, respectively, led to good agreement with the measured temperatures. It is worth noting that, in some sedimentary rocks, the thermal conductivity in the direction parallel to the bedding plane is more than twice higher than that in the direction perpendicular to the bedding plane (Midttømme et al., 1996). After Schön (1996), the reasons for this anisotropy in thermal conductivity of sedimentary rocks are: (i) crystal anisotropy of the individual rock-forming minerals; (ii) intrinsic or structural anisotropy resulting from the mineral shapes and their textural arrangement within the rock; (iii) orientation and geometry of crack fractures and other defects. Point (ii) is particularly true in the case of clays and claystones because of the planar shape of clay platelets and the bedding orientation by long term consolidation, creep and diagenesis.

In addition to anisotropy, the presence of the Excavation Damage Zone (EDZ) around underground constructions can also influence the thermal conductivity. However, few studies have been devoted to this aspect.

Three methods are often used to measure the thermal conductivity of soils in the laboratory: i) the divided bar method, ii) the needle probe method (or line source method) and iii) optical scanning. The divided bar method is a steady state method in which a constant temperature gradient is imposed across the sample, resulting in a stable heat flow. This method involves heat transmission along a single direction only, and is considered to be accurate (Johansen, 1975; Farouki, 1981; Brigaud et al., 1990; Midttømme and Roaldset, 1999). It is also recommended to be used in measuring the thermal conductivity of rock samples (Beck, 1988; Ashwroth, 1990). The needle probe method is a transient method in which a radial heat flow is produced within the specimen while measuring temperature changes over time. This method is based on the theory of axisymmetric heat diffusion from an infinite line source within an infinite surrounding medium. It is valid when the ratio between the length and the diameter of the needle is larger than 30:1 (Popov et al., 1999). The thermal conductivity can hence be back calculated from the temperature-time curve (Jessop, 1990). In the optical method (Popov, 1983), a focused, mobile and continuously operated heat source is used to heat a sample while

monitoring temperature changes using infrared temperature sensors. The excess temperatures monitored on the sample are compared to that of a reference sample of known thermal conductivity, allowing the thermal conductivity to be determined. This method has been recommended to estimate the thermal anisotropy of rocks (Popov et al., 1999).

In this paper, the needle probe method was selected for its simplicity and standardisation. The thermal anisotropy of Boom Clay was investigated by adopting various orientations of the needle with respect to the bedding orientation of the samples. These experimental results were then compared with the theoretical results. The Boom Clay samples were extracted from a series of cores taken from a horizontal borehole drilled from a gallery of the HADES URL. The core was at 2.40 m to 22.3 m distance to the gallery axis (HADES borehole 2012-2 / Connecting Gallery / Ring 66-67W) and the specimens were extracted from the core at various distances ranging from 2.5 to 20.8 m to the gallery axis.

2 Background

2.1 Anisotropy of thermal conductivity

Heat flow by conduction along one dimension is governed by Fourier's law:

$$q = -\lambda \frac{dT}{dx} \tag{2}$$

where q is the heat flux density (W/m^2), λ is the thermal conductivity (W/(m.K)) and dT/dx is the temperature gradient along the x direction.

In an anisotropic material, the apparent thermal conductivity λ measured on an anisotropic sample around a line-source is related to the principal components of the thermal conductivity tensor (Grubbe et al., 1983; Popov et al., 1999), as follows:

$$\lambda = \sqrt{\lambda_A \lambda_B \cos^2(\gamma) + \lambda_A \lambda_C \cos^2(\beta) + \lambda_B \lambda_C \cos^2(\alpha)} \tag{3}$$

where, λ_A, λ_B and λ_C are the three principal components of the thermal conductivity tensor; α, β and γ are the angles between the line-source axis and the principal directions of thermal conductivity tensor

A, B and C, respectively (Fig. 1). Knowing the angles α, β and γ in equation (3), the apparent thermal conductivity λ can be determined through three measurements.

Due to the stratification and bedding, many sedimentary rocks and clays are transversely isotropic, leading to the following relations: $\lambda_A = \lambda_\perp$ (thermal conductivity in the direction perpendicular to the bedding plane) and $\lambda_B = \lambda_C = \lambda_{//}$ (thermal conductivity in the direction parallel to the bedding plane). If the axis of the emitting needle probe is perpendicular to the bedding plane (Fig. 1a), $\alpha = 0°$ and $\beta = \gamma = 90°$. Hence:

$$\lambda_0 = \sqrt{\lambda_B \lambda_C \cos^2(0°)} = \lambda_{//} \tag{4}$$

When the needle is parallel to the bedding plane (Fig. 1b), $\alpha = \gamma = 90°$, $\beta = 0°$ and λ represents λ_{90}:

$$\lambda_{90} = \sqrt{\lambda_A \lambda_C \cos^2(0°)} = \sqrt{\lambda_\perp \lambda_{//}} \tag{5}$$

From (4) and (5):

$$\lambda_\perp = \frac{(\lambda_{90})^2}{\lambda_0} \tag{6}$$

Equation (6) has been used by several authors (Penner, 1963; Munroe and Sass, 1987; Popov et al., 1999; Pribnow et al., 2000; Gong, 2005; Davis et al., 2007; Popov et al., 2012; Riche and Schneebeli, 2012) to determine the value of thermal conductivity in the direction perpendicular to bedding $\lambda_\perp$ based on the measurements of λ_{90} and λ_0 in different materials (clay sediments, igneous rocks, snow, etc.).

In general, when the line source axis forms an angle θ with the normal to the bedding (Fig. 1c), an apparent thermal conductivity can be determined by:

$$\lambda_\theta = \sqrt{\lambda_\perp \lambda_{//} \sin^2(\theta) + (\lambda_{//})^2 \cos^2(\theta)} \tag{7}$$

Thus,

$$\lambda_\theta = \sqrt{(\lambda_0)^2 \cos^2(\theta) + (\lambda_{90})^2 \sin^2(\theta)} \tag{8}$$

Equation (8) was firstly proposed by Pribnow (cited by Davis et al., 2007). This function was used to compare the experimental results with the changes in probe orientation. The data of Davis et al. (2007) agree reasonably well with equation (8).

To calculate the value for $\theta = 45°$, substituting equation (6) into equation (8) yields:

$$\lambda_{45} = \sqrt{\frac{\left[(\lambda_0)^2 + (\lambda_{90})^2\right]}{2}} \tag{9}$$

2.2 Thermal conductivity at saturated state

Various authors stated that the thermal conductivity of clays depends on several factors such as the composition (solid, water and gas phases), the nature of the dominant minerals, the density/porosity, the temperature, etc. (Farouki, 1986; Clauser and Huenges, 1995; Midttømme and Roaldset, 1999; Tang et al., 2008). In this study, the effects of the slight changes in degree of saturation (S_r) and density of the investigated samples were taken into account based on the Johansen's method (Farouki, 1986). According to Johansen, the thermal conductivity of an unsaturated soil is a function of its thermal conductivity at dry and saturated states at the same dry density. To establish this function, Johansen (1975) introduced a normalized thermal conductivity, namely Kersten's number (K_e):

$$K_e = (\lambda - \lambda_{dry}) / (\lambda_{sat} - \lambda_{dry}) \tag{10}$$

where λ_{sat} is the thermal conductivity at saturated state, λ is the thermal conductivity at intermediate degree of saturation, λ_{dry} is the thermal conductivity at dry state

Hence, one can deduce the saturated thermal conductivity value from the thermal conductivity measurement conducted on non-saturated samples, according to the following relationship:

$$\lambda_{sat} = \frac{(\lambda - \lambda_{dry})}{K_e} + \lambda_{dry} \tag{11}$$

In fine-grained unfrozen soils, Johansen proposes the following relationships for K_e and λ_{dry}:

$$K_e \cong \log S_r + 1.0 \tag{12}$$

$$\lambda_{dry} = \frac{0.135\rho_d + 64.7}{2700 - 0.947\rho_d} \pm 20\% \ (W/(m.K)) \tag{13}$$

where ρ_d is the dry density in kg/m^3.

3 Material and methods

3.1 The Boom Clay

In Belgium, researches on geological radioactive waste disposal in clay formation were initiated by SCK•CEN in 1974. The first Underground Research Laboratory (URL) HADES was then excavated in Boom Clay formation at a depth of 223 m during the early Eighties at a site close to the city of Mol and has been progressively extended since. The Boom Clay was chosen as a potential host rock for radioactive waste disposal due to its very low permeability (its hydraulic conductivity around 2.10^{-12} m/s and 5.10^{-12} m/s in the direction perpendicular and parallel to the bedding, respectively), its capacity to retard the migration of many radionuclides by sorption, its high plasticity, and its capacity of self-sealing after physical disturbances.

Located at 190 m - 290 m below ground level at Mol (ONDRAF/NIRAS, 2001), Boom Clay was deposited during the Tertiary Era about 30 millions years ago. The Boom Clay layer is almost horizontal with a slight 1-2% north-east dip. It is located between water-bearing sand layers (ONDRAF/NIRAS, 2001).

In order to investigate both the anisotropy in thermal conductivity of Boom Clay and the possible influence of the excavation damaged zone (EDZ) on it, nine samples were taken at various distances from the gallery (4.0 m in diameter, 0.4 m in liner thickness) from the core (100 mm in diameter) taken from a borehole (reference number: R66-67/2012) drilled horizontally till approximately 22 m in length, in July 2012. Once drilled, the core was immediately sealed under vacuum in aluminium foils to minimize drying effects. Table 1 summarizes the physical properties of the nine samples. The distance to the gallery axis r varies from 2.5 m to 20.8 m. The water content of the samples (w) slightly changes from 22.6% to 24%, which is in the range of the in- situ measurements (from 22% to 27%). The densities are comparable (1630-1640 kg/m^3) except for the sample that was the closest to the gallery (TH6, r = 2.9 m, ρ_d = 1.61 Mg/m^3). A suction measurement was made on sample TH11 (r = 9.60 m) using a chilled mirror hygrometer (WP4, Decagon Device), and a value of 2.8 MPa was

obtained, in good agreement with the suction value reported in Delage et al. (2007) from a sample at the same depth.

3.2 Thermal conductivity measurements

The apparatus used to measure the thermal conductivity is a commercial handheld device named KD2 Pro Thermal Properties Analyzer (Decagon Devices, Inc.). The kit consists of a controller and 3 separated sensors (small single needle, large single needle, dual needle) that can be inserted into the tested medium. The small single needle (60 mm in length, 1.3 mm in diameter) (Fig. 2b) was used to measure the thermal conductivity of Boom Clay. The accuracy of the thermal conductivity measurement using this needle is ±5% from 0.2 W/(m.K) - 2 W/(m.K).

Cylindrical samples were trimmed from cores (100 mm in diameter and 60mm - 90 mm in height). The bedding orientation that could be identified from direct visual observation was marked. The samples were then slightly confined by means of an adhesive tape so as to avoid further crack propagation and any perturbation.

Three holes were prepared in each sample by drilled in each sample using a drilling-machine (Fig. 2a) equipped with a thin steel drill (1.3 mm in diameter, 65 mm in effective length). In order to ensure a good thermal contact between specimen and probe, the needle probe was coated with a thin layer of thermal grease (high-density polysynthetic silver thermal compound by Arctic Silver) prior to its insertion into the drilled hole (Fig. 2b), as recommended by the ASTM standard D5334-08 (2008). For a better precision, it was decided to run 5 successive measurements at intervals of 15 minutes.

The measured thermal conductivity values were denoted λ_0, λ_{45} and λ_{90}, defined by the value of the angle θ between the axis of the hole and the direction normal to the bedding (see Fig. 1 and Fig. 3). As mentioned previously, heat transfer in the case of $\theta = 0°$ is parallel to the bedding (Fig. 1a), and the λ_0 value measured by the needle device is equal to the thermal conductivity in the direction parallel to the bedding ($\lambda_{//}$). In the two other cases, the measured values depend on the thermal conductivities in the

directions parallel and perpendicular to the bedding. The thermal conductivity in the direction perpendicular to the bedding ($\lambda_{\perp}$) needs to be back calculated, as seen in the previous section.

4 Experimental results

4.1 Anisotropy of thermal conductivity

Since the degrees of saturation of the nine specimens are slightly lower than 100% (see Table 1), the thermal conductivities at saturated state were first calculated using equation (11). As seen in Table 2 in which the initial ($\lambda_{//0}$) and corrected $\lambda_{//}$ values are presented, the corrections made for saturation are small with a relative variation ($\Delta\lambda_{//}/\lambda_{//0}$) included between 0.64% and 2.04%. The values of thermal conductivity in the direction perpendicular to the bedding at saturated state $\lambda_{\perp}$ were afterwards determined using equation (6) based on the value of λ_{90} determined from a test with the needle parallel to the bedding (Fig. 3). The thermal conductivity anisotropy ratio η was then deduced from equation **Erreur ! Source du renvoi introuvable.**.

4.2 Influence of EDZ on thermal conductivity

The changes in thermal conductivity along the three directions (λ_0, λ_{45}, λ_{90}, Fig. 3) with respect to the distance to the gallery axis *r* are shown in Fig. 4. The gallery wall is also represented in this figure. The vertical bars indicate the range of the 5 measurements performed on each sample. The calculated values of λ_{45} (from λ_0 and λ_{90} using equation (9)) are also plotted for comparison with the test data directly obtained using the needle probe inclined at 45° with respect to the bedding. Excellent agreement was observed, confirming: (i) 2D anisotropy model (presented in the part 2.1), (ii) correspondence of principal axes of thermal conductivity to bedding plane orientation shown in Figure 1.

Fig. 4 shows that all the measurements start from a low value in the zone close to the gallery wall (around 1.3 W/(m.K) for $\lambda_0 = \lambda_{//}$ at r = 2.5 m). The conductivity values increase with distance to reach a maximum value at around 6.4 m from the gallery axis (1.6 W/(m.K) for $\lambda_{//}$). A slight decrease ($\lambda_{//}$) or a more significant one ($\lambda_{\perp}$) is observed for samples taken at greater distances from the gallery (up to

20.8 m). The average value of 1.6 W/(m.K) for $\lambda_{//}$ observed at larger distances is in good agreement with the value of 1.65 W/(m.K) obtained from the back calculations carried out within the ATLAS III project (Chen et al., 2011; Yu et al., 2011).

These results also confirm that the thermal conductivity in the direction parallel to the bedding is always higher than that in the direction perpendicular to the bedding. The values of $\lambda_{//}$ vary between 1.34 - 1.61 W/(m.K) whereas those of $\lambda_{\perp}$ vary between 0.82 – 1.06 W/(m.K) (Fig. 4). This can also be observed in Fig. 5 that presents the changes in anisotropy ratios η versus the distance r to the gallery axis. The values of η change between 1.5 and 1.8 with no significant effect of the distance to the gallery axis. Note that the value of $\lambda_{\perp}$ obtained in this study is smaller than that obtained by back calculations (1.31 W/(m.K)) by Chen et al. (2011). This difference may be explained by the fact that $\lambda_{\perp}$ is much more dependent on confinement (that strongly affects the contact between parallel clay particles) than $\lambda_{//}$. Further studies on the effect of confinement on the anisotropic thermal conductivity are needed to confirm this point.

5 Discussion

It is now well recognized that an Excavation Damaged Zone (EDZ) characterized by a fracture network including shear and tension fractures along with a herringbone pattern of fractures develops during excavation in clays and claystones (Mertens et al., 2004; Bastiaens and Mertens, 2005; Davies and Bernier, 2005; Tsang et al., 2005; Bernier et al., 2007; Tsang et al., 2012; Armand et al., 2013). The extent of this zone depends on various parameters such as the nature of the media (soft clay, stiff clay or claystone), its mechanical properties, the excavation technique, the state of stress around the gallery and the bedding orientation. Around the Connecting Gallery of the URL HADES at Mol, an EDZ characterized by a herringbone fracture pattern has been observed (Bastiaens and Mertens, 2005; Bernier et al., 2007) with open fractures extending to about 1 m from the gallery wall. There were indications that the extent in the horizontal direction was somewhat larger than in the vertical direction.

The thermal conductivity measurements carried out in this study on samples extracted from a horizontal borehole at various distances from the gallery axis evidenced changes that can be related to the EDZ, given that discontinuities are suspected to affect heat transfer across these. In this regard, the thermal conductivity changes in the direction parallel to the bedding ($\lambda_{//}$) seems to be the more significant parameter to be considered since the borehole was horizontal with a sub-vertical orientation of cracks in this area. Indeed, inspection of Fig. 4 shows that parameter $\lambda_{//}$ starts from small values to afterwards increase with the distance to the gallery (until a distance *r* of 4.0 m from the gallery axis, corresponding to about 1.6 m from the outside wall). Beyond this distance, the horizontal thermal conductivity remains about constant, around a value of 1.6 W/(m.K), in good accordance with the back analysis of the in-situ heating test. Based on the thermal conductivity measurements, it is deduced that the EDZ extension in the horizontal direction is about 1.6 m from the outside of gallery's wall, a value in consistence with in situ observation.

The data presented here were obtained from the laboratory measurements carried out on samples extracted from a horizontal core and under zero confining stress. As a result, there would be some possibility of cracks' opening within the samples due to stress release. Thereby, the effects of cracks on thermal fluxes observed in Fig. 4 could be enhanced by the stress release. Thus, the question arises as to whether the changes in thermal conductivity with respect to the distance to the gallery really occur in-situ. Actually, clays are known to exhibit self-sealing properties with respect to water transfer. This self-sealing behaviour, interpreted as the recovery of a good contact between the two faces of discontinuities, could have comparable consequence on heat transfer as well. In other words, self-sealing could be extended from fluid transfer to heat transfer. Such a hypothesis should obviously be further investigated by thermal conductivity measurements in the laboratory, under confining conditions and/or running detailed in-situ measurement at various distances from the gallery completed by thermal back-analysis of in-situ thermal tests. Meanwhile, the changes in thermal conductivity carried out here on laboratory samples provide a complementary identification of the extent of the EDZ along a horizontal direction around the gallery excavated in Boom Clay.

6 Conclusion

An experimental study using the needle thermal probe technique was conducted for investigating the thermal conductivity anisotropy of natural Boom Clay. The investigation was carried out on samples extracted from a series of cores (from a single borehole) taken from the Underground Research Laboratory at Mol in Belgium, at a depth of 223 m. Thermal conductivity was measured on specimens sampled at various distances to the gallery axis, from 2.5 to 20.8 m. Measurements were conducted along three directions: parallel, perpendicular and at an angle of 45° with respect to the bedding plane. A significant thermal anisotropy was evidenced and data confirmed that the highest conductivity was in the direction parallel to bedding and that the smallest one was in the direction perpendicular to bedding, the one at 45° being logically in between these two values. It is worth noting that the conductivity values found in this laboratory study in the direction parallel to the bedding was close to that back-calculated from the in-situ ATLAS experiments (Chen et al., 2011).

The effect of an excavation damaged zone (EDZ) was also evidenced: the thermal conductivity in the three directions increased with the distance to the gallery. Based on the experimental data, an EDZ extent of about 1.6 m in the horizontal direction was identified, a value consistent with the in situ observation. Finally, the thermal anisotropy did not appear to be significantly affected by the excavation damage, with no significant effect of the distance to the gallery on the thermal anisotropy ratio that was comprised between 1.48 and 1.74.

Acknowledgements

The authors are grateful to Ecole des Ponts ParisTech (ENPC), the European Underground Research Infrastructure for Disposal of nuclear waste In Clay Environment (EURIDICE) and the Belgian agency for radioactive waste management (ONDRAF/NIRAS) for their financial support.

References

ANDRA, 2005. Dossier 2005 Argile. Synthesis - Evaluation of the feasibility of a geological repository in an argillaceous formation, December 2005.

343 Armand, G., Leveau, F., Nussbaum, C., de La Vaissiere, R., Noiret, A., Jaeggi, D., Landrein, P., and
344 Righini, C., 2013. Geometry and Properties of the Excavation-Induced Fractures at the
345 Meuse/Haute-Marne URL Drifts. Rock Mechanics and Rock Engineering, DOI:
346 10.1007/s00603-012-0339-6.

347 Ashworth, T., Ashworth, E., and Ashworth, S. F., 1990. New apparatus for use with materials of
348 intermediate conductivity, Thermal conductivity 21 Edited by C. Cremers and A. Fine, Plenum
349 Press, New York, 51-66.

350 Bastiaens, W. and Mertens, J., 2005. EDZ around an industrial excavation in Boom Clay, Proceedings
351 of a European Commission Cluster Conference and Workshop, 305-309, C. Davies and F.
352 Bernier (eds), Luxemburg, 3-5 November 2003, European Commission .

353 Beck, A.E., 1988. Methods for determining thermal conductivity and thermal diffusivity. In: Haenel,
354 R., Rybach, L. & Stegena, L. (eds) Handbook of Terrestrial Heat Flow Density Determination.
355 Kluwer, Dordrecht, 87-124.

356 Bernier, F., Li, X. L. and Bastiaens, W., 2007. Twenty-five years' geotechnical observation and
357 testing in the Tertiary Boom Clay formation. Géotechnique (57)2, 229-237.

358 Brigaud, F., Chapman, D.. and Le Douaran, S., 1990. Estimating thermal conductivity in sedimentary
359 basins using lithological data and geophysical well logs. Bulletin, American Association of
360 Petroleum Geologists, 74, 1459-1477.

361 Buntebarth, G., 2004. Bestimmung thermophysikalischer Eigenschaften an Opalinustonproben,
362 Geophysikalisch-Technisches Büro, Clausthal-Zellerfeld.

363 Chen, G. J., Sillen, X., Verstricht, J., & Li, X. L., 2011. ATLAS III in situ heating test in Boom Clay:
364 Field data, observation and interpretation. Computers and Geotechnics, 38(5), 683–696.
365 doi:10.1016/j.compgeo.2011.04.001.

366 Clauser, C., and Huenges, E., 1995. Thermal Conductivity of Rocks and Minerals. In: T. J. Ah-rens
367 (ed), Rock Physics and Phase Relations - a Handbook of Physical Constants, AGU Reference
368 Shelf, Vol. 3, pp. 105-126, American Geophysical Union, Washington

369 D5334-08, 2008. Standard Test Method for Determination of Thermal Conductivity of Soil and Soft
370 Rock by Thermal Needle Probe Procedure.

371 Davies, C. and Bernier, F., 2005. Impact of the excavation disturbed or damaged zone (EDZ) on the
372 performance of radioactive waste geological repositories. Proceedings of a European
373 Commission Cluster Conference and Workshop, Luxemburg, 3-5 November 2003, European
374 Commission.

375 Davis, M.G., Chapman, D.S., Van Wagoner, T.M., & Armstrong, P. A., 2007. Thermal conductivity
376 anisotropy of metasedimentary and igneous rocks. Journal of Geophysical Research, 112(B5), 1–
377 7. doi:10.1029/2006JB004755.

378 Delage, P., Le, T.-T., Cui, Y.-J., Tang, A.-M., Li, X.-L., 2007. Suction effects in deep Boom Clay
379 block samples. Géotechnique, 57(2), 239–244. doi:10.1680/geot.2007.57.2.239

380 Farouki, O.T., 1981. Thermal Properties of Soils. Cold Region Research and Engineering Laboratory
381 Monograph 81-1.

382 Farouki, O.T., 1986. Thermal properties of soils (Series in Rock and Soil Mechanics vol.11). Trans
383 Tech Publications, Clausthal-Zellerfeld, Germany.

Gong, G., 2005. Physical properties of alpine rocks: a laboratory investigation. Thèse de doctorat: Univ. Genève, no. Sc. 3658.

Grubbe, K., Haenel, R., Zoth, G., 1983. Determination of the vertical component of thermal conductivity by line source methods. Zeitblatt für Geologie und Palaontologie. Teil I H (1/2), 49-56.

Jessop, A.M., 1990. Thermal Geophysics. Elsevier, Amsterdam.

Jobmann, M., Polster, M., 2007. The response of Opalinus clay due to heating: A combined analysis of in situ measurements, laboratory investigations and numerical calculations. Phys. Chem. Earth, Parts A/B/C 32, 929–936.

Johansen, O., 1975. Varmeledningevne av jordarter. Dr.ing avhandling, institutt for kjoleteknikk, Norwegian Institute of Technology (NTH), Trondheim. (Thermal conductivity of soils. PhD thesis, Cold Region Research and Engineering Laboratory (CRREL) Draft Translation 637, 1977, ADA 044002, Hanover, NH.

Mertens, J., Bastiaens, W., and Dehandschutter, B., 2004. Characterisation of induced discontinuities in the Boom Clay around the underground excavations (URF, Mol, Belgium). Applied Clay Science, 26(1-4), 413–428. doi:10.1016/j.clay.2003.12.017

Midttømme, K., Roaldset, E., Brantjes, J.G., 1996. Thermal conductivity of alluvial sediments from the Ness Formation, Oseberg Area, North Sea. EAEG 58th Conference, Extended Abstracts Volume 2, P552.

Midttømme, K., Roaldset, E., 1999. Thermal conductivity of sedimentary rocks: uncertainties in measurement and modeling. Geological Society, London, Special Publications, 158: 45-60, doi:10.1144/GSL.SP.1999.158.01.04.

Mügler, C., Filippi, M., Montarnal, P., Martinez, J.-M., Wileveau, Y., 2006. Determination of the thermal conductivity of Opalinus Clay via simulations of experiments performed at the Mont Terri underground laboratory. J. Appl. Geophys. 58, 112–129.

Munroe, R.J, and Sass J.H., 1987. Thermal conductivity of samples from borehole VC-1, Report 87-184, Geological Survey.

ONDRAF/NIRAS, 2001. ONDRAF/NIRAS, SAFIR2 – Safety Assessment and Feasibility Interim Report 2, ONDRAF/NIRAS report NIROND 2001-06E.

Penner, E., 1963. Anisotropic thermal conduction in clay sediments. International Clay Conference.

Popov, Y.A., Pribnow, D.F.C., Sass, J.H., Williams, C.F., & Burkhardt, H., 1999. Characterization of rock thermal conductivity by high-resolution optical scanning. Geothermics, *28*(2), 253–276. doi:10.1016/S0375-6505(99)00007-3.

Popov, Y., Bayuk, I., Parshin, A., Miklashevskiy, D., Novikov, S., Chekhonin, E., 2012. New methods and instruments for determination of reservoir thermal properties, in: Proceedings Thirty-Seventh Workshop on Geothermal Reservoir Engineering. Stanford University, Stanford, California.

Popov, Y.A., 1983. Theoretical models of the method of determination of the thermal properties of rocks on the basis of movable sources. Geologiya i Razvedka (Geology and Prospecting) Part I, 9, 97-103 (in Russian).

Pribnow, D.F.C., Davis, E.E., Fisher, A.T., 2000. Borehole heat flow along the eastern flank of the Juan de Fuca Ridge, including effects of anisotropy and temperature dependence of sediment thermal conductivity, Geological Survey of Canada.

Riche, F., and Schneebeli, M., 2012. Thermal conductivity of anisotropic snow measured by three independent methods. The Cryosphere Discussions, 6(3), 1839–1869. doi:10.5194/tcd-6-1839-2012.

Schön, J.H., 1996. Physical Properties of Rocks: Fundamentals and Principles of Petrophysics Volume 18 of Handbook of geophysical exploration: Seismic exploration. Elsevier, Oxford.

Tang, A.-M., Cui, Y.-J., Le, T.-T., 2008. A study on the thermal conductivity of compacted bentonites. Applied Clay Science, 41(3-4), 181–189. doi:10.1016/j.clay.2007.11.001.

Tsang C.F., Bernier F. and Davies C., 2005. Geohydromechanical processes in the EDZ in crystalline rock, rock salt and indurated and plastic clays – in the context of radioactive waste disposal. International Journal of Rock Mechanics and Mining Sciences, 42, 109-125

Tsang C.F., Barnichon J.D., Birkholzer J., Li X.L., Liu H.H. and Sillen X., 2012. Coupled thermo-hydro-mechanical processes in the near field of a high-level radioactive waste repository in clay formations. International Journal of Rock Mechanics and Mining Sciences 49, 31-44.

Yu, L., Weetjens, E. and Vietor, T., 2011. Integration of TIMODAZ Results within the Safety Case and Recommendations for Repository Design. External report SCK-CEN-ER-188, SCJ-CEN, Mol, Belgium.

Yu, L., Weetjens, E., Sillen, X., Vietor, T., Li, X.L., Delage, P., Labiouse, V., and Charlier, R., 2013. Consequences of the Thermal Transient on the Evolution of the Damaged Zone Around a Repository for Heat-Emitting High-Level Radioactive Waste in a Clay Formation: a Performance Assessment Perspective. Rock Mechanics and Rock Engineering. doi:10.1007/s00603-013-0409-4.

List of Tables

Table 1: Properties of natural Boom Clay samples taken at various distances togallery axis (ρ_d : dry density, w: water content, e: void ratio, S_r : degree of saturation) .

Table 2: Initial and corrected $\lambda_{//}$ values ($\lambda_{//0}$: thermal conductivity measured on non-saturated samples, Corrected $\lambda_{//}$: saturated thermal conductivity after Johansen's method, $\Delta\lambda_{//}$: difference between the $\lambda_{//0}$ and Corrected $\lambda_{//}$).

List of Figures

Fig.1: Principal axes of thermal conductivity for the three cases studied with the needle probe method. A, B and C: main (orthogonal) axes of thermal conductivity (A is perpendicular to the bedding plane; B and C are parallel to the bedding plane).

Fig.2: Running a test by the needle probe method (a): system for drilling; (b) inserting the needle probe into the specimen with marks of the bedding plane.

Fig.3: Measurement of thermal conductivity.

Fig.4: Thermal conductivity versus distance r to the axis of the gallery.

Fig.5: Degree of thermal conductivity anisotropy versus distance r to the axis of the gallery.

Table 1: Properties of natural Boom Clay samples taken at various distances r to gallery axis (ρ_d : dry density, w: water content, e: void ratio, S_r : degree of saturation)

Test	Distance r (m)	ρ_d (kg/m^3)	w (%)	e	S_r (%)
TH6	2.5	1610	23.98	0.65	97.9
TH7	2.6	1640	23.05	0.63	98.0
TH8	2.7	1640	23.05	0.63	98.0
TH14	3.4	1630	23.51	0.64	98.4
TH13	3.8	1630	23.02	0.63	98.0
TH12	6.0	1630	22.84	0.64	95.2
TH11	9.2	1640	22.63	0.63	96.3
TH10	16.0	1640	22.61	0.63	96.2
TH9	20.8	1630	23.48	0.64	98.4

Table 2: Initial and corrected $\lambda_{//}$ values ($\lambda_{//0}$: thermal conductivity measured on non-saturated samples, Corrected $\lambda_{//}$: saturated thermal conductivity after Johansen's method, $\Delta\lambda_{//}$: difference between the $\lambda_{//0}$ and Corrected $\lambda_{//}$).

Tests	Distance r (m)	S_r	$\lambda_{//0}$ (W/(m.K))	Corrected $\lambda_{//}$ (W/(m.K))	$\Delta\lambda_{//}$ / $\lambda_{//measured}$) (%)
TH6	2.5	97.9	1.33	1.34	0.85
TH7	2.6	98.0	1.38	1.39	0.80
TH8	2.7	98.0	1.41	1.42	0.80
TH14	3.4	98.4	1.45	1.46	0.64
TH13	3.8	98.0	1.54	1.55	0.81
TH12	6.0	95.2	1.56	1.59	2.04
TH11	9.2	96.3	1.58	1.61	1.55
TH10	16.0	96.2	1.49	1.51	1.57
TH9	20.8	98.4	1.52	1.53	0.67

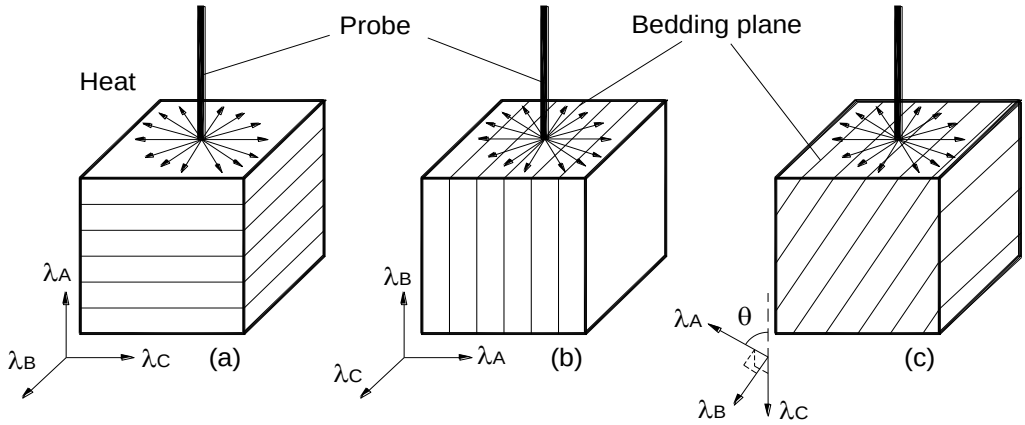

Fig. 1: Principal axes of thermal conductivity for the three cases studied with the needle probe method. A, B and C: main (orthogonal) axes of thermal conductivity (A is perpendicular to the bedding plane; B and C are parallel to the bedding plane).

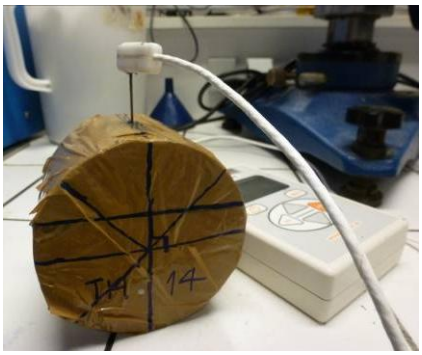

(a) (b)

Fig. 2 : Running a test by the needle probe method (a): system for drilling; (b) inserting the needle probe into the specimen with marks of the bedding plane.

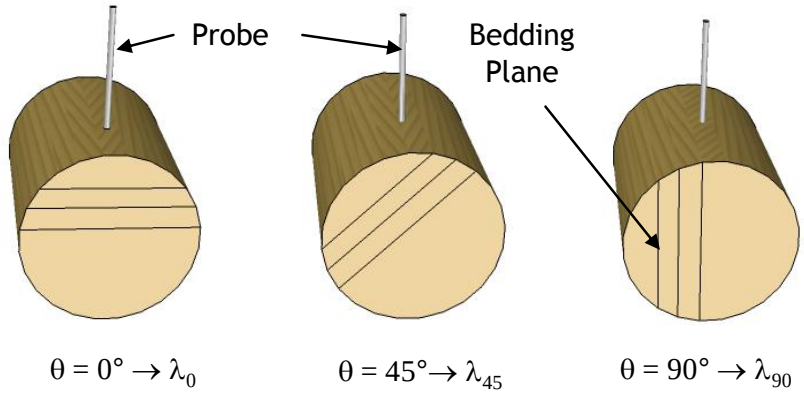

500

501 Fig. 3 : Measurement of thermal conductivity.

502

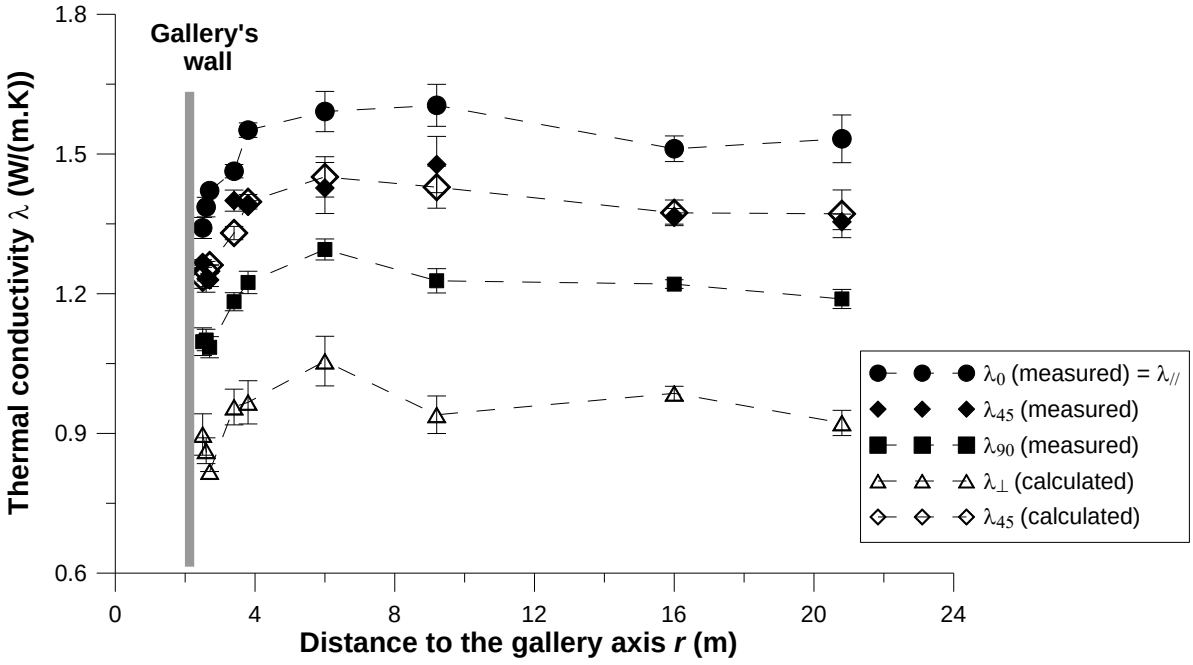

503

504 Fig. 4: Thermal conductivity versus distance *r* to the axis of the gallery.

505

506

507

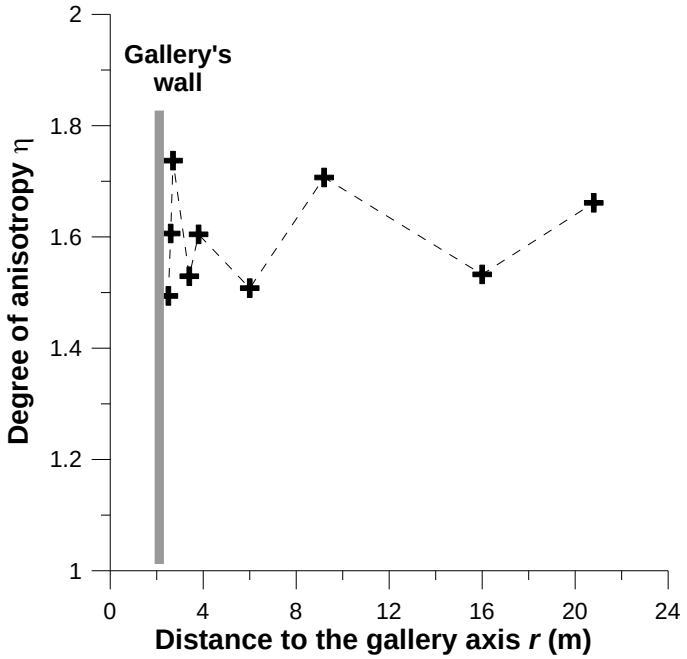

508

509 Fig. 5: Degree of thermal conductivity anisotropy versus distance *r* to the axis of the gallery.

510

511
512